



TITLE:

Kinetics of cubic to tetragonal transformation under external field by the time-dependent Ginzburg-Landau approach

AUTHOR(S):

Ichitsubo, T; Tanaka, K; Koiwa, M; Yamazaki, Y

CITATION:

Ichitsubo, T ...[et al]. Kinetics of cubic to tetragonal transformation under external field by the time-dependent Ginzburg-Landau approach. PHYSICAL REVIEW B 2000, 62(9): 5435-5441

ISSUE DATE:

2000-09-01

URL:

<http://hdl.handle.net/2433/50118>

RIGHT:

Copyright 2000 American Physical Society

Kinetics of cubic to tetragonal transformation under external field by the time-dependent Ginzburg-Landau approach

Tetsu Ichitsubo,^{1,*} Katsushi Tanaka,¹ Masahiro Koiwa,¹ and Yoshihiro Yamazaki²

¹*Department of Materials Science and Engineering, Kyoto University, Kyoto 606-8501, Japan*

²*Institute for Nonlinear Sciences and Applied Mathematics, Hiroshima University, Higashi-Hiroshima 739-8526, Japan*

(Received 27 March 2000; revised manuscript received 26 May 2000)

Computer simulations based on the time-dependent Ginzburg-Landau approach have been performed for the formation of domain structure in the cubic-tetragonal transformation under an external field. The fcc- $L1_0$ ordering has been studied as a model case of the transformation, and the Landau free-energy function has been determined so as to reproduce the free energy calculated by the Monte Carlo simulation. The simulations have demonstrated the features observed in our experiments on FePd alloy under an external stress, and have clarified the formation mechanism of a single variant structure. The internal stress field developed by the preferential formation of a variant favored by the external stress further accelerates the trend cooperatively, and eventually leads to a single variant structure.

I. INTRODUCTION

Characteristic microstructures, so-called tweed or twinned structures, have been observed frequently in various alloys which undergo cubic to tetragonal phase transformations, such as FePd, FePt, CoPt, and CuAu (fcc- $L1_0$), Ni_3V (fcc- $D0_{22}$), and martensitic FePd (fcc-fct).¹⁻⁷ In these transformations, the new phase is tetragonal and can be formed in the three different orientations with respect to the cubic mother phase. One might expect that the three variants would be formed with equal probability. The formation of tetragonal phase particles in cubic matrix, however, inevitably introduces elastic strain; random arrangements of variants would result in a large increase in the elastic energy of the system. Tweed or twinned structures can be understood as such structures in which different variants arrange themselves to reduce the elastic strain energy.

The application of an external field biases the frequency of formation of the three variants. If the effect is large enough, one favored variant would dominate in the resultant microstructure. In fact, the formation of a single variant with the tetragonal c axis parallel to the applied compressive stress or magnetic field has been observed for CoPt, CuAu, and FePd by Shimizu and Horiuchi⁸ and for FePd by the present authors.⁹⁻¹¹ Although the story apparently looks rather simple and clear, several features observed experimentally require careful examination for a better understanding of the phenomenon as listed below.

(1) The effect of an external field on the ordering of FePd appears most dominantly when the field is applied near the transition temperature. At relatively lower temperatures where the process proceeds via spinodal ordering, the application of the field does not significantly modify the process. Why?

(2) Without an external field, a pair formation of different variants resulting in a twinned structure is favored, as mentioned above. With the application of a compressive stress one type of variant is favored. At a certain level of the stress, the appearance of the second variant would be completely prohibited. The magnitude of such a stress level has been estimated in our previous work to yield a very high value of

more than 800 MPa.⁹ Experimentally, the single variant structure has been formed with far smaller stresses, 10–100 MPa. How can this discrepancy be explained?

The aim of this paper is to answer the above two questions; the result of a computer simulation study of fcc- $L1_0$ ordering under an external stress is reported. Simulations in the general case of the cubic-tetragonal transformation without external fields have been reported by Cheng *et al.*¹² and by Yamazaki.¹³ Here we perform the simulation under external stress, adopting the time-dependent Ginzburg-Landau (TDGL) approach.

II. DETERMINATION OF THE LANDAU FREE-ENERGY FUNCTION

The intention of the present simulation is a quantitative comparison with experimental observations on FePd performed in our laboratory. Therefore, the free-energy formula should be chosen so as to reproduce the actual behavior of the alloy. In a previous paper, we have calculated the free-energy variation as a function of temperature by the thermodynamic integration with Monte Carlo simulation (TIMC) method on the fcc- $L1_0$ transition,¹⁴ the result of which is used to determine the Landau free-energy function.

The coarse-grained free-energy $f(\phi)$ is assumed to have the form of the Landau type:

$$f(\phi) = \frac{\alpha(T-T_0)}{2} \phi^2 - \frac{b}{4} \phi^4 + \frac{c}{6} \phi^6, \quad (1)$$

where ϕ is the coarse-grained order parameter in the range of $-1 \leq \phi \leq 1$, T_0 is the spinodal ordering (instability) temperature, and α , b , and c are assumed to be constant. The magnitude of the eigenstrain is adopted as the order parameter ϕ . The square of the order parameter, ϕ^2 , is zero for the fully disordered state and is unity for the fully ordered state; $0 < \phi \leq 1$ for the variant with the c axis parallel to the [010] direction (y variant), and $-1 \leq \phi < 0$ for that parallel to the [001] variant (z variant).

At the transition temperature T_t , the free energy of the ordered phase equals that of the disordered phase, and then $f(\phi)$ has the following form: $\phi^2(\phi^2 - \phi_t^2)^2$, where

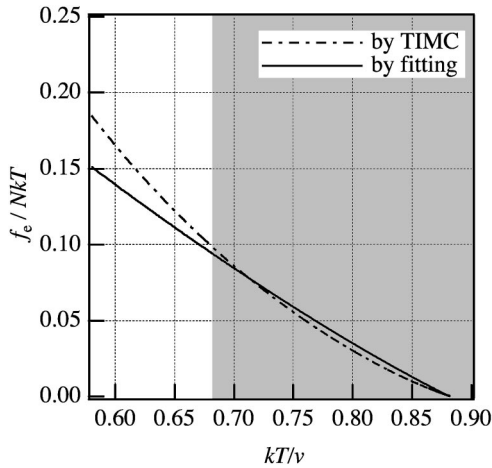


FIG. 1. The free energy calculated by the thermodynamic integration with Monte Carlo simulations (or TIMC, long and short dashed lines) and the Landau free energy fitted in the range of $0.690 \leq kT/v \leq 0.882$ (or fitting, solid line).

$\phi_t (\neq 0)$ is the order parameter at T_t . From this condition, the following relations are derived:

$$T_t = T_0 + \frac{3b^2}{16\alpha c}, \quad \phi_t^2 = \frac{3b}{4c}. \quad (2)$$

The equilibrium order parameter ϕ_e is determined from the condition $\partial f(\phi)/\partial \phi = 0$. By using ϕ_e , the free energy in the equilibrium state, f_e , is expressed as

$$f_e = f(\phi_e) = \frac{\alpha(T - T_0)}{3} \phi_e^2 - \frac{b}{12} \phi_e^4. \quad (3)$$

From the Monte Carlo simulations, the transition temperature and the spinodal ordering temperature have been determined to be $kT_t/v \approx 0.882$ (Ref. 14) and $kT_0/v \approx 0.708$ (see the Appendix), respectively, where v is the nearest-neighbor effective interaction energy and k is the Boltzmann constant. Since the eigenstrain is empirically proportional to the square of the long-range order parameter,¹⁵ the order parameter ϕ_t at T_t is given by $\phi_t = \eta_t^2 \approx (0.850)^2$. By substituting the above values into Eq. (2), the coefficients b and c can be expressed in terms of α : $f_e = f(\alpha, T)$. Then, the value of α is determined so as to best reproduce the free-energy difference evaluated by the TIMC method.¹⁴

Figure 1 shows the free-energy difference by the TIMC method and the free energy by Eq. (3) fitted in the range of $0.690 \leq kT/v \leq 0.882$ (the shaded area). The Landau free-energy function can be written as

$$\begin{aligned} \frac{f(\phi)}{NkT} = & 0.746 \left(\frac{kT}{v} - 0.708 \right) \phi^2 - 0.497 \phi^4 \\ & + 0.475 \phi^6 - \sigma_{mn}^A \varepsilon_{mn}^*(\phi), \end{aligned} \quad (4)$$

where N is the number of atoms, the last term $-\sigma_{mn}^A \varepsilon_{mn}^*(\phi)$ is the mechanical interaction energy, σ_{mn}^A is the external stress field, and $\varepsilon_{mn}^*(\phi)$ is the eigenstrain tensor. Figure 2 shows the Landau free-energy curves at T_t and at T_0 without the external stress field.

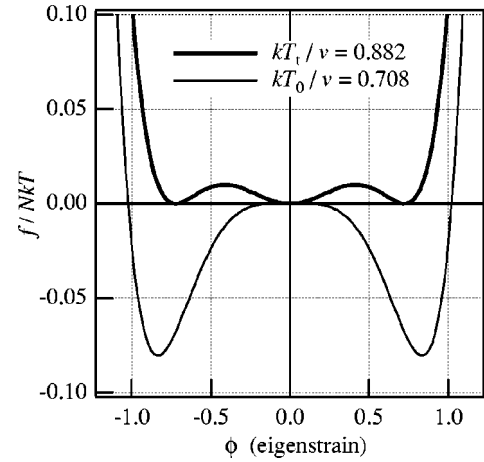


FIG. 2. The fitted Landau free-energy as a function of the order parameter. The reduced temperature $kT/v = 0.882$ is the transition temperature and $kT/v = 0.708$ is the spinodal ordering temperature for the fcc/ $L1_0$ transition.

For the fcc- $L1_0$ transition without a change in the lattice volume, the eigenstrain $\varepsilon_{mn}^*(\phi)$ of each variant is given by

$$\varepsilon_{mn}^{*(y)} = \varepsilon_0 \phi \begin{pmatrix} 1 & 0 & 0 \\ 0 & -2 & 0 \\ 0 & 0 & 1 \end{pmatrix} = \varepsilon_0 \phi T_{mn}^{(y)}, \quad (\phi > 0), \quad (5)$$

$$\varepsilon_{mn}^{*(z)} = \varepsilon_0 \phi \begin{pmatrix} -1 & 0 & 0 \\ 0 & -1 & 0 \\ 0 & 0 & 2 \end{pmatrix} = \varepsilon_0 \phi T_{mn}^{(z)}, \quad (\phi < 0), \quad (6)$$

where ε_0 represents the magnitude of the tetragonality of the fully ordered state, and (y) and (z) indicate the kinds of variants.

III. COMPUTER SIMULATION

A. Kinetic equation

The kinetic process is assumed to be governed by the following TDGL (Langevin) equation:

$$\frac{\partial \phi(\mathbf{r}, t)}{\partial t} = -L \frac{\delta F\{\phi\}}{\delta \phi} + \theta(\mathbf{r}, t), \quad (7)$$

where L is the relaxation rate and $\theta(\mathbf{r}, t)$ is the thermal noise (fluctuation) at a position \mathbf{r} and time t . Since the free energy consists of the chemical energy and the elastic energy, the Ginzburg-Landau free-energy functional F is given by

$$F\{\phi\} = \int d\mathbf{r} \left[f(\phi(\mathbf{r})) + \frac{K_S}{2} |\nabla \phi(\mathbf{r})|^2 + f_{el}(\phi(\mathbf{r})) \right], \quad (8)$$

where K_S is the gradient coefficient. The elastic strain energy function f_{el} is given by

$$f_{el} = \frac{1}{2} C_{pqmn} [\varepsilon_{pq}^*(\phi(\mathbf{r})) - \gamma_{pq}(\phi(\mathbf{r}))] \varepsilon_{mn}^*(\phi(\mathbf{r})), \quad (9)$$

where C_{pqmn} are the elastic constants, and $\varepsilon_{pq}^*(\phi(\mathbf{r}))$ and $\gamma_{pq}(\phi(\mathbf{r}))$ are the eigenstrain and the constrained strain as-

TABLE I. The parameters used for the simulations.

	f_e [MJ/m ³]	K_S [J/m]	Δd [nm]	$L \times \Delta t$ [m ³ /J]
723 K	-64.7	5.64×10^{-12}	0.5	$10^{-10} \times 1$
823 K	-34.2	6.33×10^{-12}	0.5	$10^{-10} \times 1$
	c_{11} [GPa]	c_{12} [GPa]	c_{44} [GPa]	$\varepsilon_0 \phi_e$
723 K	182	135	71.5	± 0.0126
823 K	174	129	68.7	± 0.0119

sociated with the formation of an ordered domain with the order parameter ϕ , respectively.¹⁶

In the elastic equilibrium, $\gamma_{pq}(\mathbf{r})$ is given by

$$\gamma_{ik}(\mathbf{r}) = \sum_{\xi \text{ space}} \left[\frac{1}{2} C_{jlmn} \bar{\xi}_l (G_{ij}^{-1} \bar{\xi}_k + G_{kj}^{-1} \bar{\xi}_i) \hat{\varepsilon}_{mn}^*(\xi) \right] \times \exp \left(i \frac{2\pi}{M} \xi \cdot \mathbf{r} \right), \quad (10)$$

where $G_{ij} = C_{ipjq} \bar{\xi}_p \bar{\xi}_q$, $\bar{\xi}$ is the unit vector of ξ ,^{17,18} M is the division number of the system for the discrete Fourier transformation, and $\hat{\varepsilon}_{mn}^*(\xi)$ is the Fourier transformation of $\varepsilon_{mn}^*(\mathbf{r}')$.

The partial differential of the strain energy function f_{el} with regard to ϕ is given by

$$\frac{\partial f_{el}}{\partial \phi} = \frac{\partial f_{el}}{\partial \varepsilon_{mn}^*} \frac{\partial \varepsilon_{mn}^*}{\partial \phi} = -\sigma_{mn} \varepsilon_0 T_{mn}^{(y \text{ or } z)}, \quad (11)$$

where σ_{mn} is the internal stress field given by $C_{pqmn}(\varepsilon_{pq}^* - \gamma_{pq})$, and $T_{mn}^{(y)}$ or $T_{mn}^{(z)}$ are chosen depending upon the value of ϕ : for $\phi(\mathbf{r}, t) > 0$ or $\phi(\mathbf{r}, t) < 0$, respectively. Then, the TDGL (Langevin) equation is given by

$$\frac{\partial \phi}{\partial t} = -L \left[\frac{\partial f}{\partial \phi} - \sigma_{mn} \varepsilon_0 T_{mn}^{(y \text{ or } z)} - K_S \nabla^2 \phi \right] + \theta. \quad (12)$$

B. Parameters and procedure

The parameters used for the simulations are chosen to represent the properties of the equiatomic Fe-Pd alloy system, as listed in Table I. In the fcc- $L1_0$ transformation, the ordering can proceed in either of two distinct ways: one is the nucleation and growth process at relatively high temperatures, $T > T_0$, and the other is the spinodal ordering process at relatively low temperatures, $T < T_0$. As the transition temperature is 923 K ($kT_0/v \approx 0.882$), T_0 is estimated to be 741 K ($kT_0/v \approx 0.708$). The simulations have been performed at two temperatures, 823 K ($kT/v = 0.786 > T_0$) and 723 K ($kT/v = 0.691 < T_0$). The tetragonality constant ε_0 is set at 0.015, and then the eigenstrain component $\varepsilon_0 \phi_e$ in the equilibrium state is ± 0.0126 at 723 K and is ± 0.0119 at 823 K.

The free energy per unit volume is obtained by multiplying Eq. (4) by NkT/V_m , where $V_m \approx 8.32 \times 10^{-6}$ [m³/mol]. In the calculation of the strain energy, Eq. (10) has been calculated by the fast Fourier transformation technique under the conditions of the periodic boundary and the plane strain in the [100] direction (i.e., $\gamma_{11} = \gamma_{12} = 0$); the elastic con-

stants of the ordered phase are assumed to be the same as those of the disordered phase of FePd alloy¹⁹. The system is divided into 64×64 areas [i.e., $M = 64$ in Eq. (10)], and the divided grid distance is set at $\Delta d = 0.5$ [nm]. The gradient coefficient K_S is approximately expressed as $K_S \approx 2\gamma_s \Delta d / \phi_e^2$, and γ_s is assumed to be 4 mJ/m², arbitrarily.

Equation (12) has been solved numerically by the Euler technique:

$$\phi(t + \Delta t) = \phi(t) - \Delta t \frac{L}{\Omega} \frac{\partial(f + f_{el})\Omega}{\partial \phi} + \Delta t \frac{L}{\Omega} (K_S \nabla^2 \phi) \Omega + \int_t^{t+\Delta t} \theta dt', \quad (13)$$

where Ω is the coarse-grained volume. The unit time step and the relaxation rate are set at $\Delta t = 1$ and $L = 10^{-10}$ [m³/J Δt], respectively. The thermal noise $\int_t^{t+\Delta t} \theta dt'$ is given by the Gaussian random number with a zero average and variance s_θ^2 ; the variance of the thermal noise is often assumed to satisfy the relation

$$s_\theta^2 = 2 \frac{L}{\Omega} kT \Delta t = 2L^* kT \Delta t, \quad (14)$$

where $L^* (= L/\Omega)$ is the relaxation rate for the coarse-grained region. However, there exists difficulties in evaluating L^* *a priori*; therefore several small values are adopted arbitrarily for s_θ in the simulations.

All simulations have been started from the same initial state where the order parameters of the local regions are slightly deviated from $\phi = 0$.

IV. RESULTS

At temperatures where the ordering proceeds via nucleation and growth, the disordered phase, i.e., the initial state, is metastable; ordering does not occur if the thermal noise is not given ($s_\theta = 0$) in the simulation. The structure evolutions simulated at 823 K with a thermal noise of $s_\theta = 0.02$ are shown in Fig. 3(a) (without stress) and Fig. 3(b) (with stress). Without the external stress, the ordered phase of the two variants (black and white regions) and the fcc disordered phase (gray region) coexist. The ordered domains are nearly aligned in the $\langle 011 \rangle$ direction. In the earlier stage of ordering ($t = 500, 800$) a tweed pattern is formed, and then eventually develops into the twinned structure. These morphologies agree well with those reported by Yamazaki.¹³

When a uniaxial compressive stress of 100 MPa is applied, as shown in Fig. 3(b), the z variant (black region) is formed preferentially over the y variant (white region), and eventually a single domain structure is realized. Figure 4 shows the time variation of the strain energy E_S and of the volume fraction of the ordered phase V_l . Note that ordering proceeds faster under applied stress. The significant reduction of the elastic strain energy under external stress must be related to the enhancement of the ordering. The significant accumulation of elastic strain energy for the no external stress case, in contrast, accounts for the slower rate of ordering.

In our experiments, the perfectly oriented structure was obtained even when the external stress was removed at half-

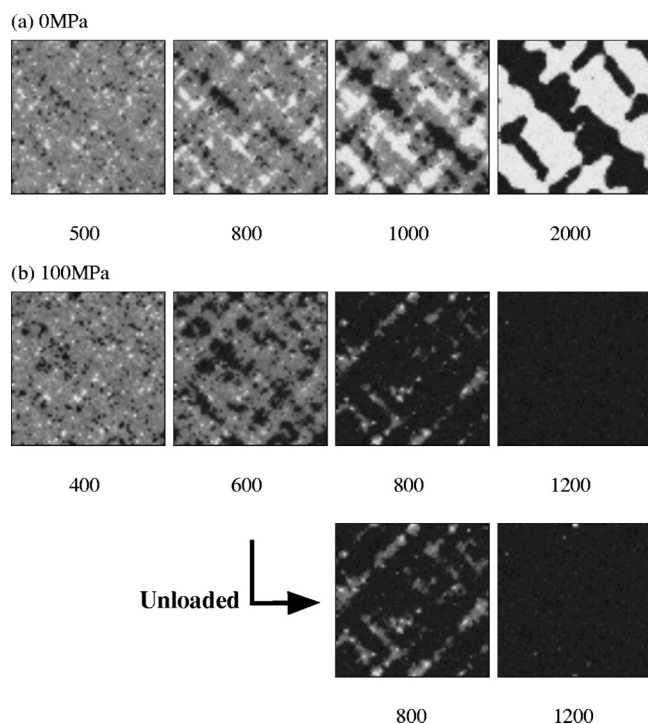


FIG. 3. Evolution of the domain structure during the ordering process at 823 K with the thermal noise $s_\theta=0.02$. (a) Without external stress and (b) with a stress of 100 MPa.

way during ordering.¹⁰ A corresponding simulation has been performed by removing the external stress at $t=600$. As shown in Fig. 3(b), the simulation reproduces successfully the trend observed experimentally; the removal of the external stress does not significantly modify the ordering rate and the reduction of the elastic strain energy (see the solid curves in Fig. 4). This feature is explained as follows: once the system is dominated by one type of variant, thereafter the single variant structure is formed spontaneously without external stress.

In the temperature range when ordering occurs in the spinodal mode, ordering in the simulation system can occur even without thermal noise $s_\theta=0$, although it seems more realistic to take into account the thermal noise. Therefore, the simulations at 723 K have been performed for both cases of $s_\theta=0$ and 0.02. First the results without thermal noise s_θ

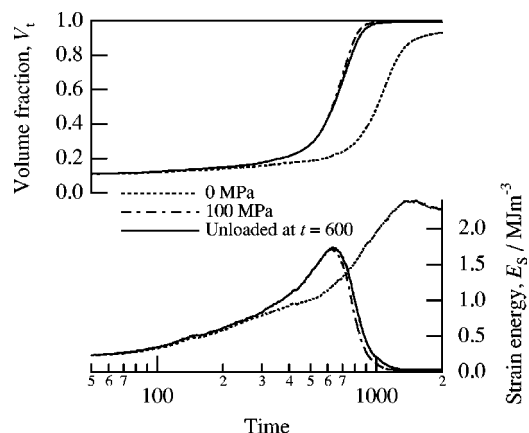


FIG. 4. The time variations of the strain energy E_S and the volume fraction V_t during the ordering process at 823 K. The solid curves show the results when the stress is removed at $t=600$.

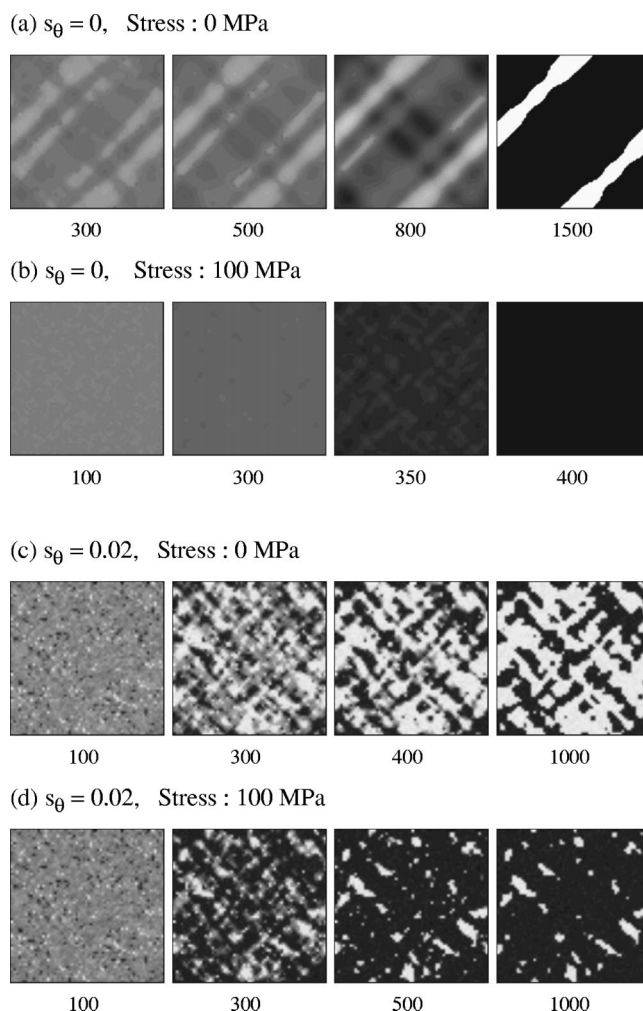


FIG. 5. Evolution of the domain structure during the ordering process at 723 K. With thermal noise $s_\theta=0$ and (a) no stress, (b) under stress (100 MPa), and with thermal noise $s_\theta=0.02$ and (c) no stress, (d) under stress (100 MPa).

$=0$ are presented in Figs. 5(a) and 5(b). Without stress, the typical tweed structure is developed, which is similar to the results reported by Cheng *et al.*¹² With a stress of 100 MPa, the system ends up in the perfectly oriented structure. This is in sharp contrast with experimental observations; the single variant structure cannot be realized in this temperature. The neglect of the thermal noise in the simulation is responsible for the discrepancy, as described below.

The results of the simulation with thermal noise $s_\theta=0.02$ are shown in Figs. 5(c) and 5(d). The oriented structure is still formed but is not so remarkable in comparison to that [Fig. 3(b)] obtained by the simulation at 823 K. This is in agreement with experimental observations. It is added here that the magnitude of the thermal noise should be changed depending upon the temperature in accordance with the relation $s_\theta^2 \propto kT$. If one adopts $s_\theta=0.02$ for 723 K, the value for 823 K should be $s_\theta=0.0213$; no significant difference has been observed in the results of two runs with $s_\theta=0.02$ and 0.0213.

V. DISCUSSION

On the basis of the results of simulations, we now discuss the two questions (1) and (2) raised in the Introduction. Fi-

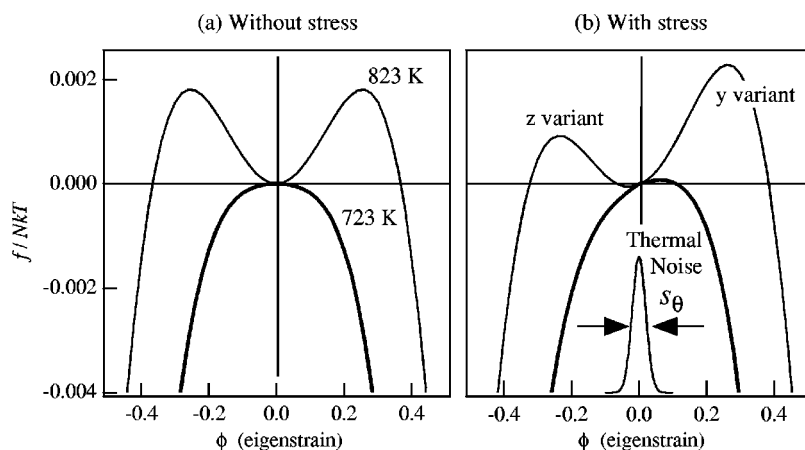


FIG. 6. The Landau free-energy curves near $\phi=0$ for the cases (a) without stress and (b) with a stress of 100 MPa. The free-energy curve is asymmetric with regard to ϕ under external stress. The solid curve is the free energy at 823 K higher than T_0 , and the bold curve is that at 723 K lower than T_0 . The thermal noise is obedient to the Gaussian distribution with a zero average and a deviation $s_\theta=0.02$.

nally, we shall remark on the limitation and prospect concerned about the TDGL (phase-field) approach.

(1) *Why is the stress effect dominant in the nucleation mode (at higher temperature)?* The change in state during ordering may be best discussed with the help of the free energy $f(\phi)$ as a function of the order parameter ϕ . Figure 6(a) shows the curves for the two representative cases of the nucleation mode (823 K) and the spinodal case (723 K). As is evident from the shape of the curve for the nucleation mode, a certain amount of thermal noise is required for the initiation of ordering. In contrast, ordering in the spinodal mode can start spontaneously; therefore, simulations are often performed without taking into account thermal noise. In principle, the thermal noise should not be ignored at all temperatures. No systematic way has been established so far to estimate a reasonable magnitude of thermal noise to be used in this kind of simulation. Thus, we have made a number of simulation runs with different magnitudes of thermal noise; the thermal noise of $s_\theta=0.02$ or around has yielded domain structures consistent with experimental observations.

Figure 6(b) shows the free-energy curves for an external stress of 100 MPa; the formation of the preferential domain structure is related to the asymmetric shape of the curve. The degree of the domination of the favorable domain, however, depends on the strength of the thermal noise adopted in the simulation. As stated above, the simulation runs have been made at two temperatures with the thermal noise of the Gaussian form (see the figure) of $s_\theta=0.02$. At the higher temperature of 823 K (the nucleation mode), the domination of the favorable variant is significant as shown in Fig. 3(b); the barrier for the formation of the y variant (unfavorable) is too high. In contrast, the barrier at 723 K (the spinodal mode) is not prohibitively high for the formation of the unfavorable variant. This is the main reason why the oriented structure develops significantly in the nucleation mode but not so much in the spinodal mode.

It is emphasized here that the simulation without thermal noise results in a structure very much different from that observed experimentally; in the spinodal mode without thermal noise, the system always favors the lower-energy state and tends to form the z variant [see Fig. 6(b)], and eventually attains at the single variant structure [see Fig. 5(b)], which is not the case observed experimentally. This demonstrates the importance of thermal noise in computer simulations to obtain realistic microstructures.

(2) *Why can a single variant structure be formed at a*

lower stress level than predicted theoretically? As stated in Sec. I, tweed or twinned structures are frequently observed in various alloy systems that undergo phase transformations from cubic to tetragonal crystals. The structure can be understood as the formation of pairs of different variants in close vicinity; the elastic energy can be reduced significantly in such arrangements, in particular, for the nucleation mode where ordered domains cannot be spatially formed continuously. The application of an external stress would bias the population of variants. A simple estimate of the stress required to suppress the formation of the second variant, resulting in a single variant structure, yielded a very high value of about 800 MPa. In contradiction to the prediction, the present simulation has yielded a single variant structure under stress of 100 MPa. This is consistent with experimental observations. Moreover, the present simulation has also been successful in reproducing the following two peculiar phenomena observed experimentally: (i) the enhancement of the ordering (Fig. 4) and (ii) the formation of a single variant structure even after the removal of the external stress halfway during the ordering process [Fig. 3(b)]. These features can be understood as follows.

The favorable variant is formed very rapidly throughout the system under external stress. Then the rapid formation of the favorable variant develops a structure dominated preferentially by one type of variant. [If the applied stress is not so large, of course, the other variant can be formed due to the relaxation of the local strain, but its amount is far smaller than that of the favorable variant. See Fig. 3(b).] In such a dominated structure, a macroscopic internal stress field is developed, which can be written as $\langle\sigma_{mn}\rangle \approx V_z C_{mnik} \epsilon_{ik}^{(z)}$, where V_z is the volume fraction of the favorable variant. This internal stress accelerates cooperatively the formation of the same type of variant, because the elastic interaction energy $-\langle\sigma_{mn}\rangle \epsilon_{mn}^{(z)} < 0$. Thus, the application of external stress just triggers off the formation of the favorable variant, and the resultant internal stress field further enhances the formation of such a variant, leading to the single variant structure. This process may be said to be autocatalytic or self-organizing.

(3) *Limitation and prospect about the phase-field approach.* The TDGL simulations have been performed as quantitatively as possible in the framework of the phase-field approach. However, the results strongly depend on the magnitude of the thermal noise, as stated in paragraph (1) above. This fact indicates that the predictive capabilities of the ap-

proach are limited by the ambiguity in the evaluation of the magnitude of the thermal noise; obviously, one should exclude the ambiguity for elevating the capabilities. The magnitude of the thermal noise s_θ is closely related to the scales of time and space, as found from Eq. (14); therefore, the definitions of these scales are quite important. Here, we shall remark on these definitions.

The time scale of the simulations depends on the value of $L\Delta t$, as indicated by Eq. (13). However, the evaluation of it by a theoretical approach seems to be difficult. Therefore, $L\Delta t$ should be appropriately scaled so as to reproduce a time variation of the order parameter in a transformation process of a real alloy. Since the value of $L\Delta t$ scaled in such a way is the specific value of the alloy, let $L\Delta t$ be such a fixed value. In comparison with the definition of the time scale, that of the space scale (coarse-grained volume) is relatively easy, because the scale of spatial variation (typical domain size) can be roughly estimated when the free energy and the gradient energy are known. The essential point in the definition is that the coarse-grained scale is to be smaller than the scale of spatial variation: (i) $\Omega < (\Delta d)^2 a$, where a is the depth of a two-dimensional system ($a = \Delta d$ for a three-dimensional system). From this condition, we obtain the lower limit of the magnitude of thermal noise: $\sqrt{2LkT\Delta t}/(\Delta d)^2 a < s_\theta$.

Furthermore, as in the present case, when the aim of simulations is focused on the nucleation process, an additional condition may be adopted; the coarse-grained volume Ω is taken to satisfy that the energy fluctuation in the region Ω is smaller than the maximum of the free energy Ωf_{\max} , that is, the variation of the order parameter due to the thermal noise is smaller than the value of the order parameter ϕ_c that gives f_{\max} : (ii) $s_\theta = \sqrt{2(L/\Omega)kT\Delta t} < \phi_c \sim O(10^{-1})$. It is noted that this is an expedient condition for performing the simulations effectively.

Thus, we obtain the upper and lower limits of the magnitude of thermal noise. However, since the depth a of a two-dimensional system is not well defined, various arbitrary values can be adopted as the magnitude. This arbitrariness in the evaluation of the thermal noise is unavoidable for the two-dimensional simulations. After all, for limiting the thermal noise more uniquely, we must construct a three-dimensional model for simulations, and must define the coarse-grained volume Ω and the value of $L\Delta t$ controlling a time scale of simulations.

Finally, we add a few more words on the formula of the thermal noise. The formula is an analogy of that derived for Brownian motion. It should be noted that the formula is derived on the condition of thermal equilibrium, i.e., on the premise that the free-energy curve near the equilibrium state can be approximately written as a form of quadratic function of the order parameter. Therefore, there is no guarantee that it can be used in nonequilibrium states. When the thermal energy which causes the fluctuations of physical quantities is assumed to be virtually constant under a fixed temperature, it is unnatural that the formula be always adopted even in nonequilibrium states, because the order parameter does not fluctuate symmetrically at nonequilibrium, i.e., $|\partial f/\partial \phi| > 0$, states. It seems to be essential that the thermal noise be formulated as a yardstick of the thermal energy fluctuation in the vicinity of the equilibrium state.

VI. CONCLUSIONS

We have performed TDGL simulations of the ordering process with special attention paid to the effect of applied stress. The Landau free-energy function is constructed so as to simulate the fcc- $L1_0$ phase transformation in the equiatomic Fe-Pd alloy.

(1) It has turned out to be very important to choose a proper magnitude of thermal noise in the simulation for reproducing the microstructures observed experimentally: an oriented structure is formed in the ordering via the nucleation process (higher temperatures), but not so much in the spinodal ordering process (lower temperatures). The simulation without thermal noise in the spinodal ordering yields considerably different microstructures from those observed experimentally.

(2) The formation mechanism of a single variant structure under an external field has been clarified, as summarized below. External stress enhances the formation of one type of variant. Although the other types of variants are formed in the vicinity of the favorable variant, the population of the latter dominates so that an overall internal stress field is developed; the field is of such a nature as to enhance the formation of the domains favored by external stress. Therefore, the formation of a perfectly oriented structure is possible as a result of such an elastic interaction.

(3) For evaluating properly the thermal noise used for simulations based on the phase-field approach, the construction of a three-dimensional model system is necessarily required, and appropriate scales of space and time, i.e., the coarse-grained volume Ω and the value of $L\Delta t$, should be defined in advance.

ACKNOWLEDGMENTS

The authors wish to thank Dr. T. Koyama of Nagoya Institute of Technology for helpful suggestions and comments. This work was partly supported by a Grant-in-Aid for Scientific Research on the Priority Area Investigation of Microscopic Mechanisms of Phase Transformations for the Structure Control of Materials from the Ministry of Education, Science, Sports and Culture, Japan. One of the authors (Y.Y.) acknowledges support through the Japan Society for the Promotion of Science for Young Scientists.

APPENDIX: ESTIMATION OF THE SPINODAL ORDERING TEMPERATURE BY MONTE CARLO SIMULATIONS

The spinodal ordering temperature has been estimated by Monte Carlo simulations. Consider a system consisting of small regions of the same size. In the ordering via nucleation process, the ordered domains are formed inhomogeneously in the disordered matrix; the internal energies of the ordered regions differ from those of the disordered regions, and therefore the deviation of the internal energies increases with the formation of ordered domains, and subsequently decreases with the progress of ordering to a constant value. In contrast, in the spinodal ordering process, ordered domains are formed spatially homogeneously; the internal energy of each local region almost equals those of other local regions, and therefore the deviation of the internal energies is ex-

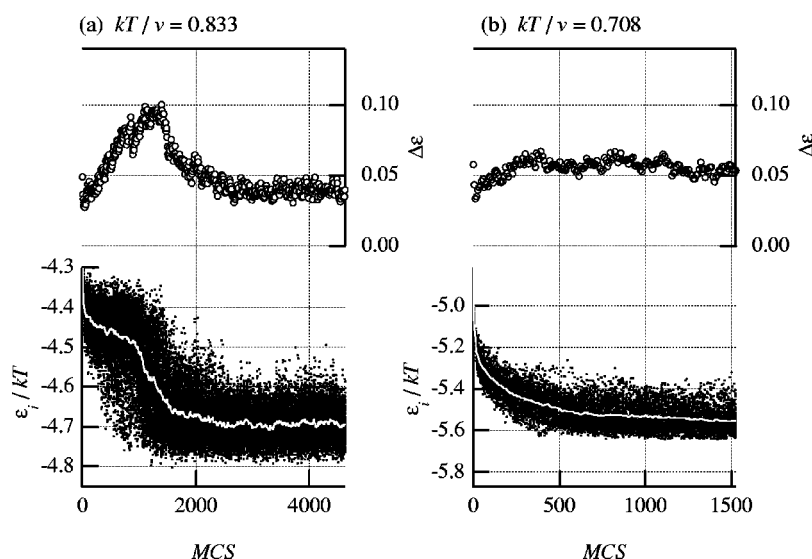


FIG. 7. The average internal energy of the system and the energies of the local regions (lower graph), and the deviation of the internal energy (upper graph) at reduced temperatures (a) 0.833 and (b) 0.708.

pected to be almost constant throughout the ordering. The spinodal ordering temperature may be defined as the temperature at which such an “increase and decrease” (i.e., maximum) of the deviation vanishes.

The model crystal, 20^3 fcc unit cells, consisting of A and B atoms with the periodic boundary condition is divided into small regions. The deviation in the internal energy of each region is given by

$$\Delta\epsilon = \sqrt{\frac{1}{M} \sum_i^M \left(\frac{\epsilon_i - \langle \epsilon \rangle}{kT} \right)^2}, \quad (\text{A1})$$

where M is the number of regions, $\langle \epsilon \rangle$ is the average internal energy, and ϵ_i is the internal energy of each region ($i = 1, 2, \dots, M$). The system was divided into 4^3 (i.e., $M = 4^3$) regions in the simulations.

The internal energy E of the system is given by vN_{AB} , where N_{AB} is the number of A-B pairs. The simulations were started from a randomly disordered state with an interchange probability $[1 - \tanh(\Delta E/2kT)]/2$, where ΔE is the change in energy produced by an exchange of two atoms.

Figures 7(a) and 7(b) show the variations (with Monte Carlo step) of ϵ_i (black dots), $\langle \epsilon \rangle$ (white dots), and $\Delta\epsilon$ (white circle) in the simulations for two temperatures, (a) $kT/v = 0.833$ and (b) $kT/v = 0.708$. For $kT/v = 0.833$ the maximum of the deviation is observed, which indicates that the ordering proceeds via the nucleation process at this temperature. In contrast, for $kT/v = 0.708$ the deviation is almost constant and the maximum is not observed, which indicates that the ordering occurs spatially homogeneously; ordering proceeds via the spinodal ordering process. Thus, the spinodal ordering temperature is roughly estimated to be $kT_0/v \approx 0.708$.

*Present address: Division of Mechanical Science, Graduate School of Engineering Science, Osaka University, Toyonaka, Osaka 560-8531, Japan. Email address: tichi@me.es.osaka-u.ac.jp

¹B. Zhang, M. Lelovic, and W. A. Soffa, *Scr. Metall. Mater.* **25**, 1577 (1991).

²R. Oshima, M. Yamashita, K. Matsumoto, and K. Hiraga, in *Proceedings of Solid-Solid Phase Transformations*, edited by W. C. Johnson, J. M. Howe, D. E. Laughlin, and W. A. Soffa (The Minerals, Metals & Materials Society, PA, 1994), p. 407.

³G. M. Guschin and F. N. Berseneva, *Phys. Met. Metallogr.* **63**, 83 (1987).

⁴M. Hirabayashi and S. Weissmann, *Acta Metall.* **10**, 25 (1962).

⁵L. E. Tanner, *Phys. Status Solidi* **30**, 685 (1968).

⁶M. Sugiyama, R. Oshima, and F. E. Fujita, *Trans. Jpn. Inst. Met.* **27**, 719 (1986).

⁷S. Muto, R. Oshima, and F. E. Fujita, *Acta Metall. Mater.* **38**, 685 (1990).

⁸S. Shimizu and S. Horiuchi, *Metall. Trans.* **1**, 330 (1970).

⁹T. Ichitsubo, M. Nakamoto, K. Tanaka, and M. Koiwa, *Mater. Trans., JIM* **39**, 24 (1998).

¹⁰T. Ichitsubo, K. Tanaka, M. Nakamoto, T. Miyoshi, and M. Koiwa, in *Proceedings of Solid-Solid Phase Transformations*, edited by M. Koiwa, K. Otsuka, and T. Miyazaki (The Japan Institute of Metals, Sendai, 1999), p. 385.

¹¹K. Tanaka, T. Ichitsubo, M. Koiwa, and K. Watanabe, *Trans. Mater. Res. Soc. Jpn.* **25**, 497 (2000); K. Tanaka, T. Ichitsubo, M. Amano, M. Koiwa, and K. Watanabe, *Mater. Trans., JIM* (to be published, Vol. 41, No. 8, 2000).

¹²L. Q. Cheng, Y. Wang, and A. G. Khachaturyan, *Philos. Mag. Lett.* **65**, 15 (1992).

¹³Y. Yamazaki, *J. Phys. Soc. Jpn.* **67**, 2970 (1998).

¹⁴T. Ichitsubo, K. Tanaka, H. Numakura, and M. Koiwa, *Phys. Rev. B* **60**, 9198 (1999).

¹⁵B. W. Roberts, *Acta Metall.* **2**, 597 (1954).

¹⁶J. D. Eshelby, *Proc. R. Soc. London, Ser. A* **241**, 376 (1957).

¹⁷A. G. Khachaturyan, *Theory of Structural Transformation in Solids* (Wiley, New York, 1983).

¹⁸N. Kinoshita and T. Mura, *Phys. Status Solidi A* **5**, 759 (1971).

¹⁹T. Ichitsubo, Ph.D. thesis, Kyoto University, 2000.